Simulation of facility effects on magnetic nozzle expansions

Diego García Lahuerta, Mario Merino, Eduardo Ahedo

Equipo de Propulsión Espacial y Plasmas (EP2),
Universidad Carlos III de Madrid, Leganés, Spain

PlasmaTech 2023

Contents

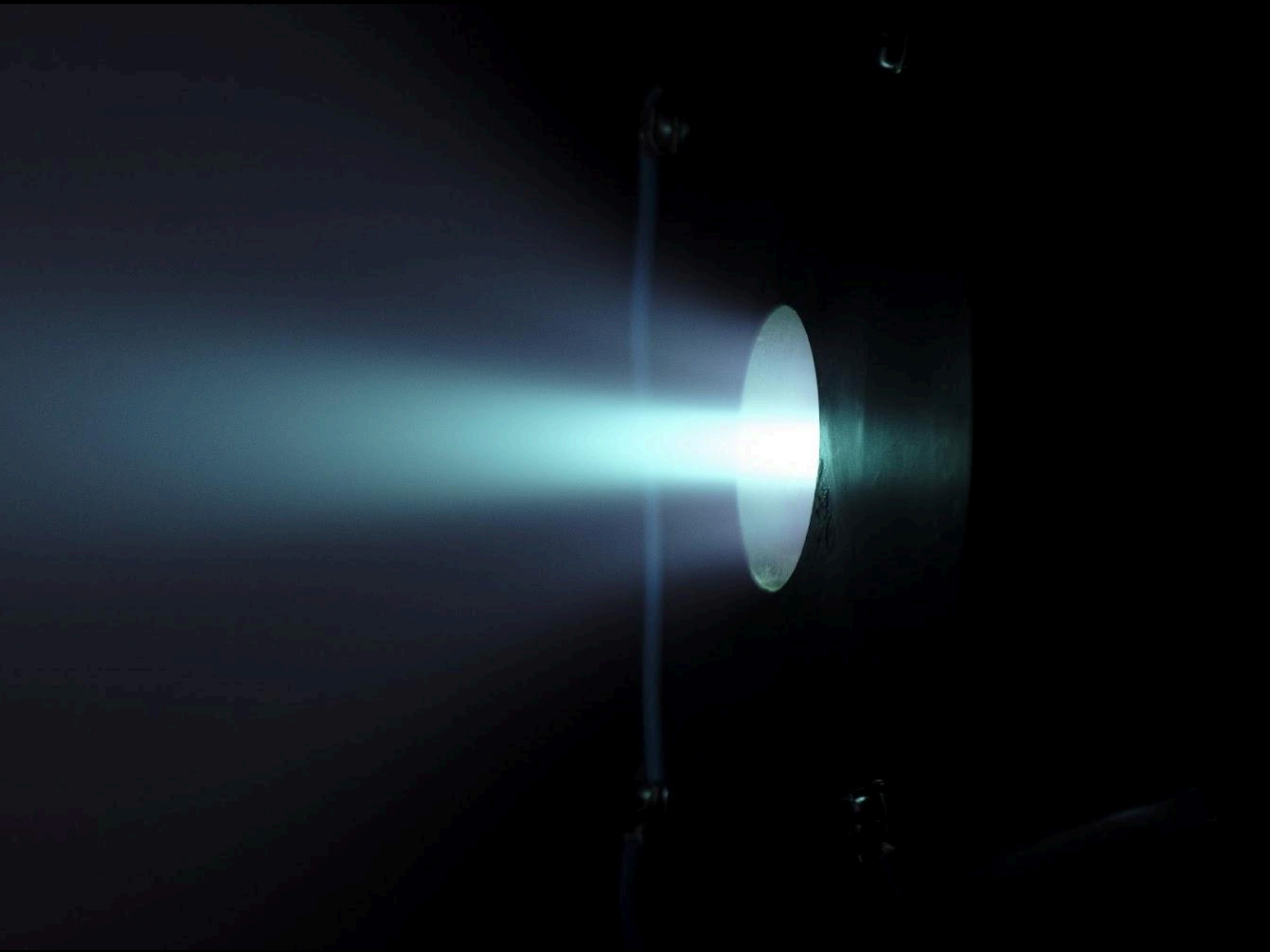

Introduction to Electric Propulsion

- Advantages over chemical propulsión:
  - Higher specific impulse
  - Higher efficiencies
  - Lower propellant mass.
- Electric Propulsion Devices:
  - Mature Technologies:
    - Gridded Ion Thruster
    - Hall Effect Thruster
  - Development:
    - Electrodeless plasma thrusters (EPTs)

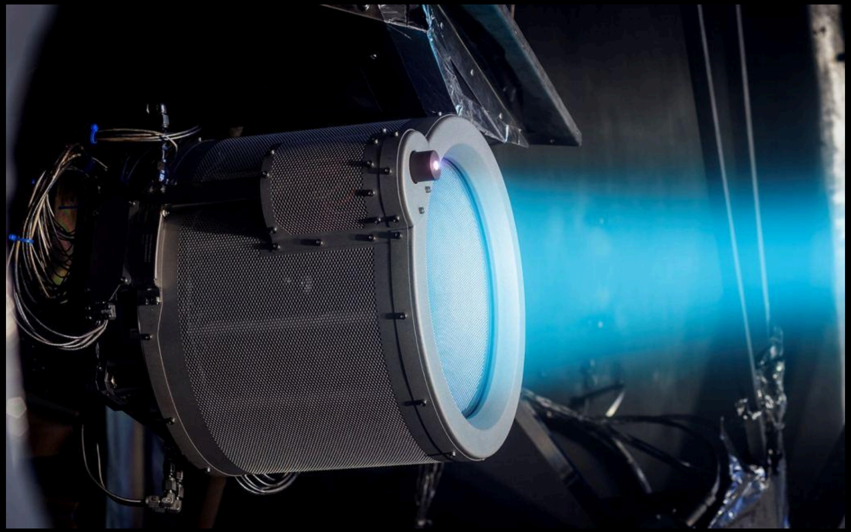

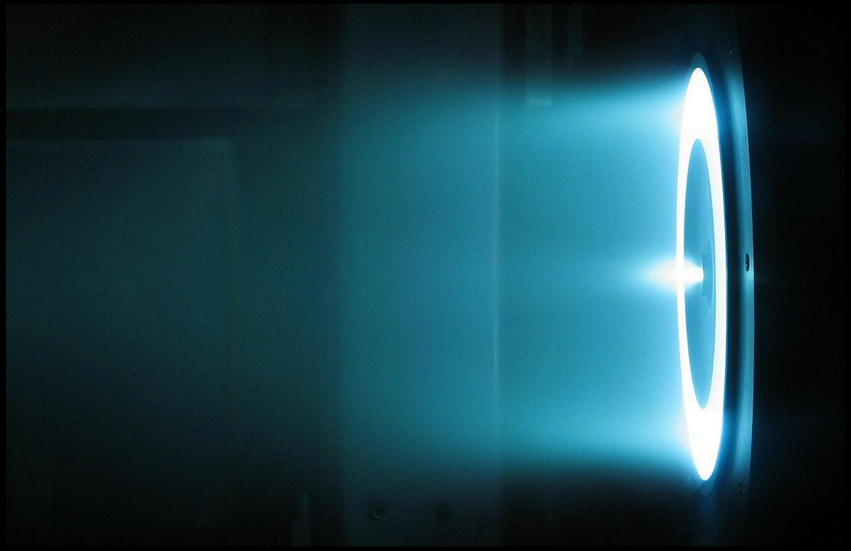

Electrodeless Plasma Thrusters

- Operational principle:
  - Energizing electrons via electromagnetic waves.
  - Acceleration of plasma in a magnetic nozzle.
- Advantages:
  - No plasma-wetted electrodes:
    - Longer thruster lifetimes.
    - Use of alternative propellants.
    - Simple electronics.
  - Better scalability to lower Powers.
- Expansion of plasma in the magnetic nozzle:
  - Convergent-Divergent magnetic field.
    - Confinement and magnetic thrust thanks to Lorentz force.
    - Convert electron thermal energy into ion kinetic energy via ambipolar electric field.
    - Detachment from closed magnetic lines downstream.

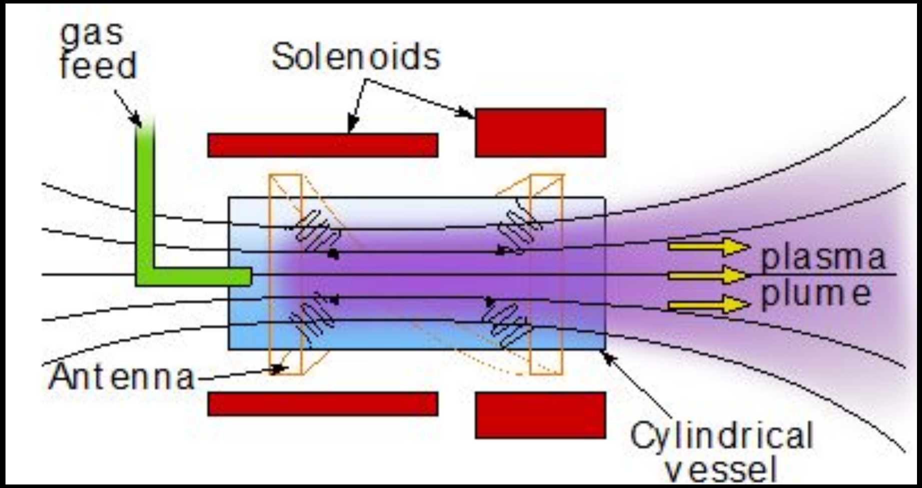

Objectives

- Ground testing of EP devices induces facility effects.
    - Effect of background pressure has been studied in other EP devices.
        - Still poor knowledge of MN response to backpressure.

- First assessment of the effect of background pressure on MN performance, taking into account late ionization in the plume.
    - Magnetic thrust.
    - Behaviour of plasma properties.

Model

- Two-Fluid Model:
  - Quasineutral plasma
  - Massless, polytropic, fully magnetized electrons.
    - $p_e = n_e^\gamma$
  - Cold, singly-charged ions
  - Ionization collisions with neutral background.
  - $\beta = 0$, negligible self induced magnetic field.

$$\frac{\partial n}{\partial t} + \nabla \cdot (n\boldsymbol{u_i}) = S$$
$$\frac{\partial n\boldsymbol{u_i}}{\partial t} + \nabla \cdot (n\boldsymbol{u_i} \otimes \boldsymbol{u_i}) = -n\,\nabla\phi + n\,\boldsymbol{u_i} \times \boldsymbol{B}$$
$$\frac{\partial n}{\partial t} + \nabla \cdot (n\boldsymbol{u_e}) = S$$
$$0 = -\nabla n T_e + n\,\nabla\phi - n\boldsymbol{u_e} \times \boldsymbol{B}$$

- Under given assumptions electron equations are found to be algebraic:
  - Electron momentum equation can be solved a priori → Thermalized potential (H_e)

$$H_e = \frac{\gamma}{\gamma - 1}(n^{\gamma-1} - 1) - \phi$$
$$u_{ye}(\psi_B) = \frac{-1}{B}\frac{\partial H_e}{\partial \mathbf{1}_\perp} = -\frac{\partial H_e}{\partial \psi_B}$$

- Ion equations are similar to Euler eqs.
  - Forcement in momentum eqs. given by:
    - Thermalized potential:
      - Encapsulates ambipolar electric field.
    - Ion magnetization, low importance.
  - Source term in continuity eq. given by collisionality.

Collision frequencies

- Collision model in continuity equation:
  - $S = \nu\, n$
- Uniform background of neutrals.
  - Only valid for low collisionalities.
- One free parameter (collision frequency).
  - Depends on:
    - Cross section.
    - Neutral density.
    - Velocity.
- Can be given by:

$$\nu = \sigma n_n v_e$$

- Typical values:
  - $\sigma \approx 10^{-19}\, m^2$
  - $p \approx 1.3 \cdot 10^{-4}\, pa \rightarrow n_n \approx 3.1 \cdot 10^{16}\, m^{-3}$
  - $v_{th} \approx 1.3 \cdot 10^6 \frac{m}{s}$
  - $\nu \approx 4.1 \cdot 10^3 s^{-1}$
  - $\nu_0 = \frac{v_0}{R_0} \approx 1.5 \cdot 10^5 s^{-1}$
- After non dimensionalization:
  - $\frac{\nu}{\nu_0} \approx 0.03$

Simulation Setup

- Numerical setup:
  - Discontinuous Galerkin discretization (FEniCS)
    - Runge Kutta time-stepping
  - Unstructured mesh (Gmsh):
    - Cell diameter such that the nozzle throat is resolved in 40 cells.
    - Order 1 elements.

- Physical parameters:
  - Gaussian density profile: $\mathrm{n}(0) = \mathrm{n}_0$ and $\mathrm{n}(\mathrm{R}_0) = 10^{-3} n_0$
  - Coil radius: $R_L = 2R_0$
  - Sonic axial velocity
  - $\gamma_e = 1.2$
  - Collisionalities: $\nu \in [0,\ 0.01,\ 0.03,\ 0.06]$

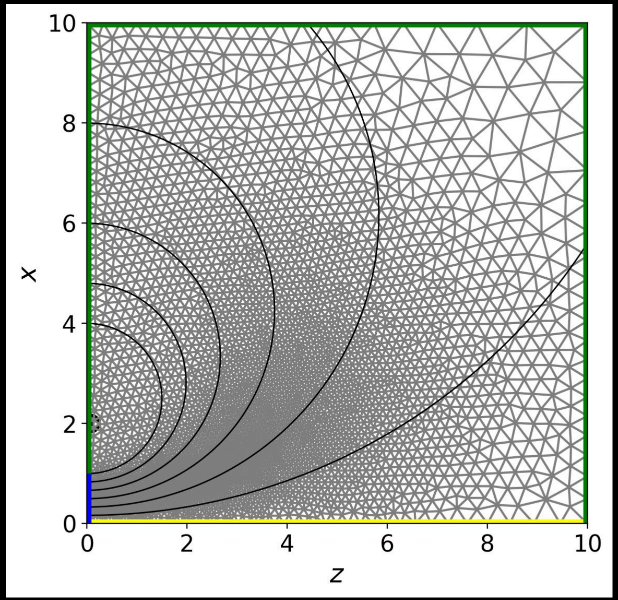

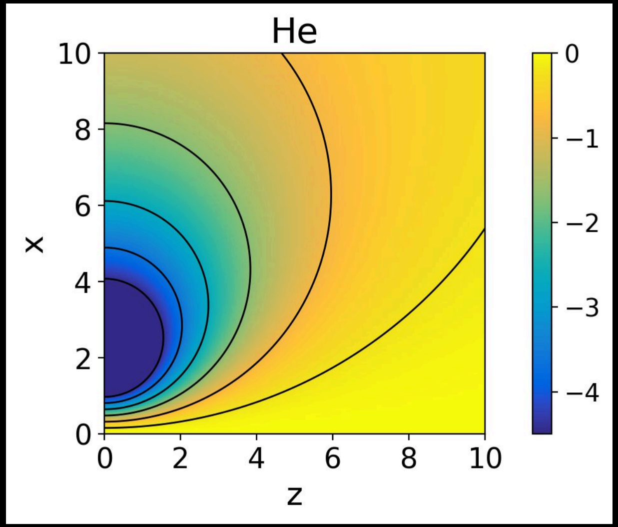

Results - Plasma Properties Maps

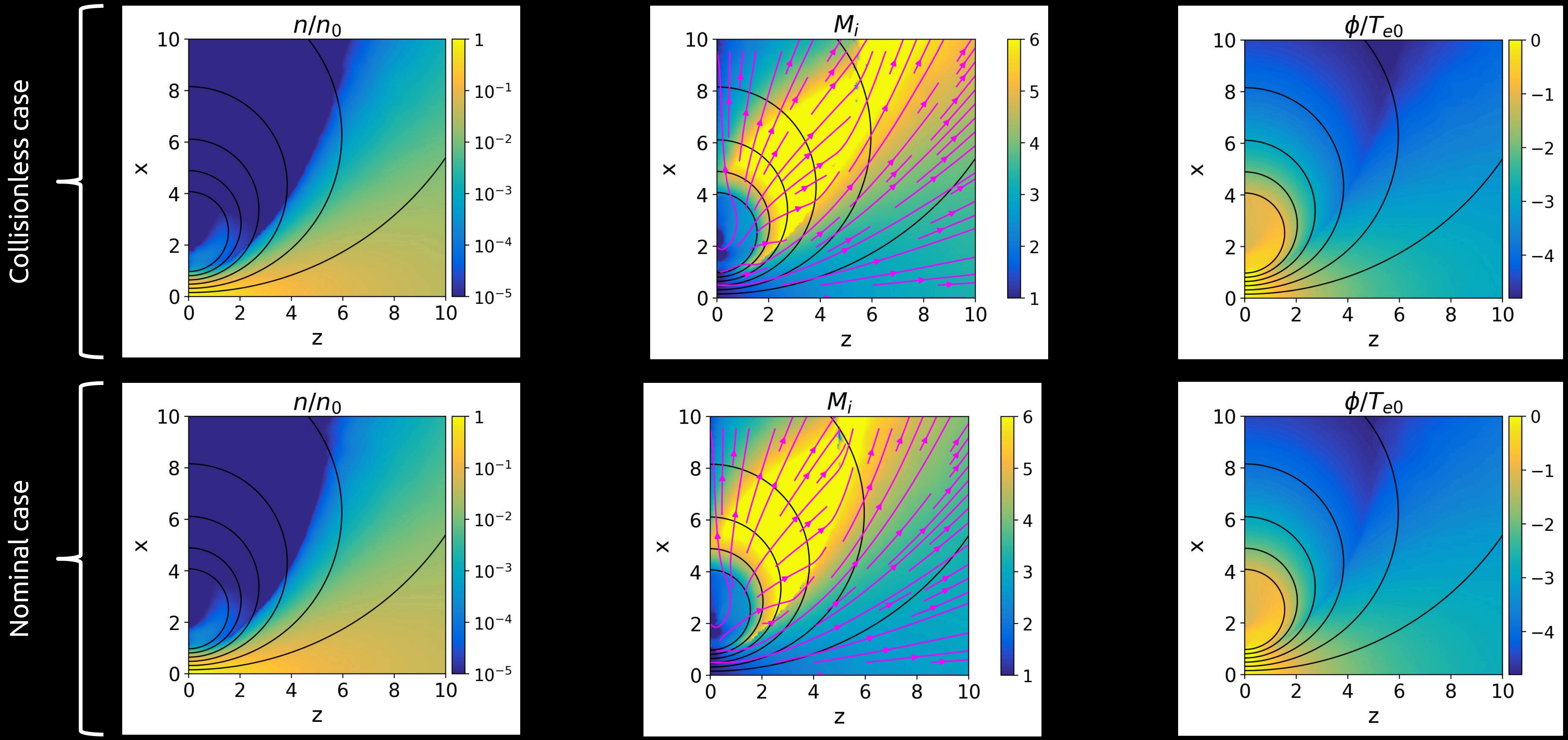

Results - Axial Behaviour

- Density at symmetry axis increases.
- Lower final ion velocity with increasing collisionality:
  - 50% drop of ion mach number over the tested ranges.
- Lower potential drop:
  - 20% drop over tested ranges.

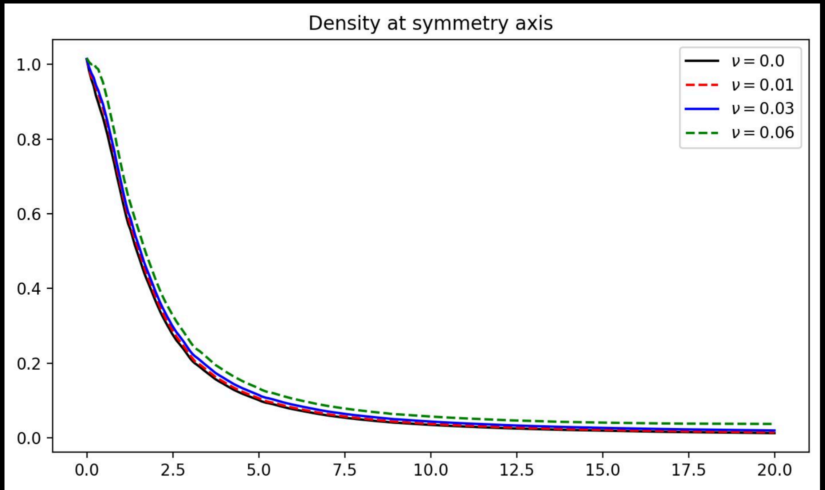

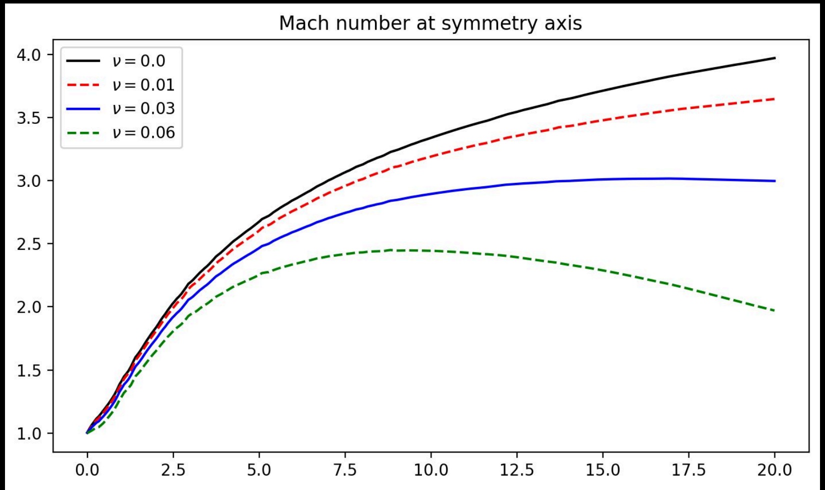

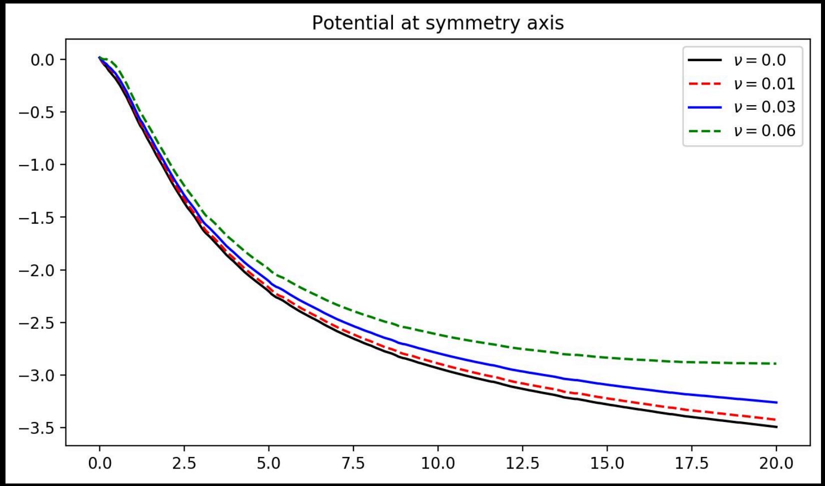

Results - Global parameters

- Total mass in the domain increases by ~ 80%
  - More plasma subject to ambipolar acceleration.
    - Total thrust increases by ~ 20%
- Stabilization of the magnetic force happens further downstream for increasing collisionality.
  - Plasma expansion takes a longer distance.

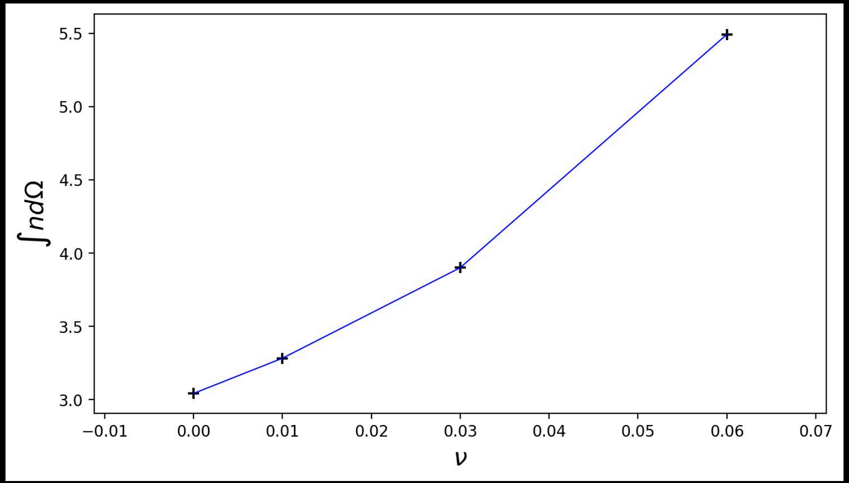

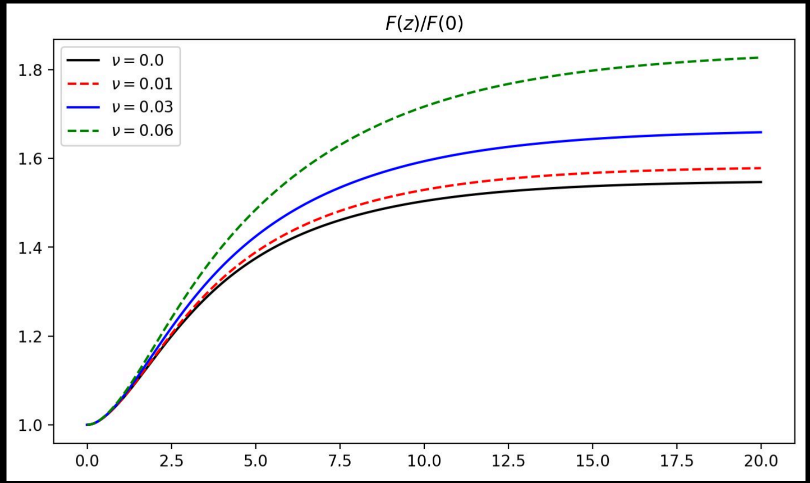

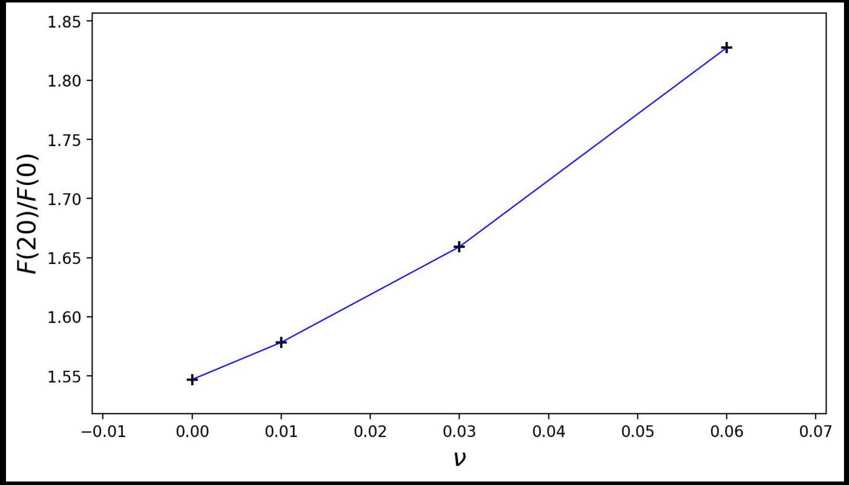

Discussion

- First step for the study of background pressure on nozzle performance.
  - Characterization of main effects on total thrust.
  - Background pressure, has a noticeable effect ion dynamics.
    - Augmented thrust due to background pressure might mask in-space behaviour.
    - Very low pressures needed for ground testing.
- Limitations:
  - Including collisions in electron momentum equations would yield lower confinement.
  - Non consistent simulation of neutrals:
    - Neutral depletion
  - Other types of collisions could also play a role:
    - CEX, excitation collisions…

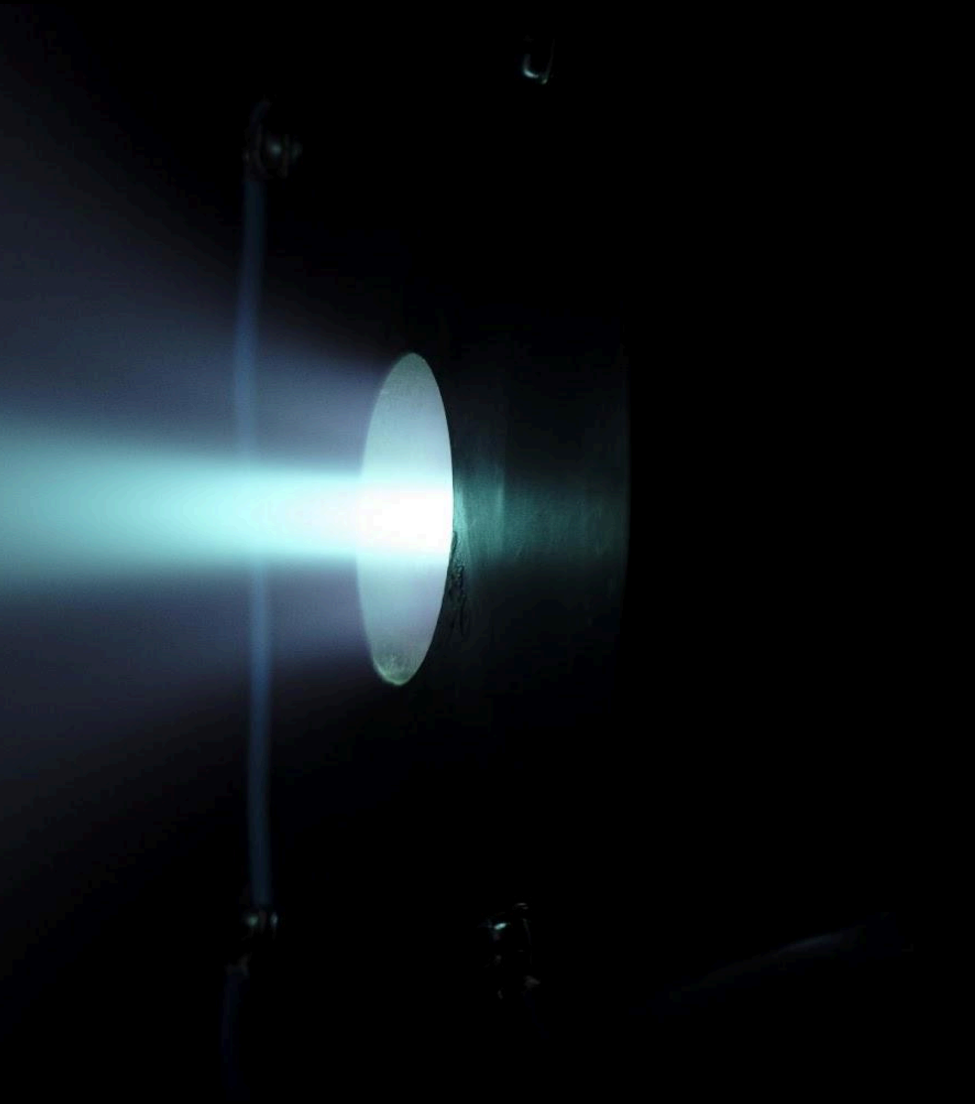

Acknowledgments

This project has received funding from the European Research Council (ERC) under the European Union's Horizon 2020 research and innovation programme (grant agreement No 950466)

European Research Council
Established by the European Commission

Thank you!

Extra Slides

Methodology: the DG-Fem method

- Finite Element Method with traits of Finite Volumes.
- Discretise the domain in k cells D_k and asume a local solution described by a polinomial.
  - Don't asume continuity at cell interfaces.
- Enforce the satisfaction of the conservation law weakly through multiplication by test functions.
- Use of a numerical flux to approximate the physical flux between discontinuous cell interfaces.

$$\partial_t u_i + \nabla_j F_{ij} = f_i$$

$$\int_{D_k} v_i\, \partial_t u_i \, d\,\Omega + \int_{D_k} v_i\, \nabla_j F_{ij} \, d\,\Omega = \int_{D_k} v_i f_i \, d\,\Omega$$

$$\int_{D_k} v_i\, \partial_t u_i \, d\,\Omega + \int_{\partial D_k} F_{ij} v_i\, n_j \, d\,\Omega - \int_{D_k} F_{ij} \nabla_j v_i \, d\,\Omega = \int_{D_k} v_i f_i \, d\,\Omega$$

$$\int_{\Omega} v_i\, \partial_t u_i \, d\,\Omega - \int_{\Omega} F_{ij} \nabla_j v_i \, d\,\Omega + \int_{\partial\Omega_{ext}} F_{ij} v_i\, n_j \, d\,s$$

$$+ \int_{\partial\Omega_{int}} H_{ij}\; n_j (v_i^+ - v_i^-) ds = \int_{\Omega} v_i f_i \, d\,\Omega$$

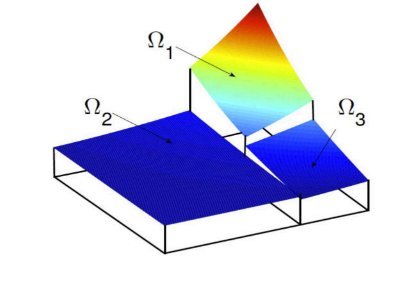

References

- E. Ahedo and M. Merino, *Physics of Plasmas* **17**, 073501(2010).
- Benjamin Wachs and Benjamin Jorns 2020 *Plasma Sources Sci. Technol.* **29** 045002(2020).
- G. Makrinich and A. Fruchtman *Physics of Plasmas* **20**, 043509 (2013).
- G. Makrinich and A. Fruchtman *Physics of Plasmas* **27**, 120601 (2020).
- M. Inchingolo, J. Navarro-Cavallé and M. Merino 2022 Direct thrust measurements of a circular waveguide electron cyclotron resonance thruster 37th Int. Electric Propulsion Conf. IEPC-2022-338.